PET/CT Versus MRI for Diagnosis, Staging, and Follow-up of Lung Cancer

Hyun Su Kim, MD,[1] Kyung Soo Lee, MD,[1] Yoshiharu Ohno, MD, PhD,[2] Edwin J.R. van Beek, MD, PhD,[3] and Juergen Biederer, MD[4]; on behalf of the 2013 International Workshop for Pulmonary Functional Imaging (IWPFI)

Positron emission tomography / computed tomography (PET/CT), with its metabolic data of ^{18}F-fluorodeoxyglucose (FDG) cellular uptake in addition to morphologic CT data, is an established technique for staging of lung cancer and has higher sensitivity and accuracy for lung nodule characterization than conventional approaches. Its strength extends outside the chest, with unknown metastases detected or suspected metastases excluded in a significant number of patients. Lastly, PET/CT is used in the assessment of therapy response. Magnetic resonance imaging (MRI) in the chest has been difficult to establish, but with the advent of new sequences is starting to become an increasingly useful alternative to conventional approaches. Diffusion-weighted MRI (DWI) is useful for distinguishing benign and malignant pulmonary nodules, has high sensitivity and specificity for nodal staging, and is helpful for evaluating an early response to systemic chemotherapy. Whole-body MRI/PET promises to contribute additional information with its higher soft-tissue contrast and much less radiation exposure than PET/CT and has become feasible for fast imaging and can be used for cancer staging in patients with a malignant condition.

J. MAGN. RESON. IMAGING 2015;42:247–260.

Evaluation of patients with suspected lung cancer comprises a diagnosis of the primary tumor and an evaluation of the extent of spread to regional or distant lymph nodes or to other structures. Structure-based imaging, using computed tomography (CT) and magnetic resonance imaging (MRI), serves as a cornerstone for the diagnosis and staging of lung cancer. In addition, it has an important role in surveillance for recurrence after surgery, assessment of response to radiotherapy or chemotherapy, and the characterization of incidental pulmonary nodule. Thus, optimal lung cancer treatment relies on accurate image-based patient analysis.

The integrated imaging adopting morphologic, functional, and metabolic datasets demonstrate synergistic effects and superiority to structure-based imaging on lung cancer evaluation. This review sets out the pros and cons of PET/CT versus MRI and will look to the future avenues we may expect from PET/MRI.

PET/CT in Lung Cancer

CT has traditionally been the standard modality of choice for the assessment of lung cancer. With advances in CT capability, this technique has enabled excellent depiction of exquisite anatomical details. However, due to several limitations, radiologists have faced challenges in diagnosing and staging of lung cancer using CT as the single imaging modality.

Over the past several decades positron emission tomography (PET), with its capability to render functional data using the glucose analog ^{18}F-fluorodeoxyglucose (FDG), has risen from being primarily a research tool to an essential imaging tool for the assessment of lung cancer.[1–3] The preferential uptake of ^{18}F-FDG into tumor cells yields a high tumor-to-background intensity ratio, which facilitates the detection of tumor foci and cellular characterization of tumor cells[4] Although PET offers high sensitivity for

View this article online at wileyonlinelibrary.com. DOI: 10.1002/jmri.24776

Received Sep 4, 2014, Accepted for publication Sep 27, 2014.

Address reprint requests to: K.S.L., Department of Radiology, Samsung Medical Center, Sungkyunkwan University School of Medicine, 50, Ilwon-Dong, Kangnam-Gu, Seoul 135-710, Korea. E-mail: kyungs.lee@samsung.com or E.J.R.v.B., SINAPSE Chair of Clinical Radiology, Clinical Research Imaging Centre, Queen's Medical Research Institute, University of Edinburgh, 47 Little France Crescent, Edinburgh EH16 4TJ, U.K. E-mail: edwin-vanbeek@ed.ac.uk

From the [1]Department of Radiology and Center for Imaging Science, Samsung Medical Center, Sungkyunkwan University School of Medicine, Seoul, Korea; [2]Division of Functional and Diagnostic Imaging Research, Department of Radiology, and Advanced Biomedical Imaging Research Centre, Kobe University Graduate School of Medicine, Kobe, Japan; [3]Clinical Research Imaging Centre, University of Edinburgh, Scotland, UK; and [4]Radiologie Darmstadt, Gross-Gerau County Hospital, Gross-Gerau, Germany

malignancy detection, it is often impossible to serve as a single imaging modality in clinical practice due to its limited spatial resolution.[1,2]

Integrated PET/CT, a dual-modality imaging system combining PET and CT in a single device, provides the fusion of PET and CT datasets obtained in a single investigation, which overcomes many of the limitations of individual CT and PET examinations.[5] The integrated imaging of morphologic and metabolic datasets shows synergistic effect for staging of lung cancer beyond an ordinary additive effect of those individual components.[2,6]

PET/CT in Solitary Pulmonary Nodule (SPN) Tissue Characterization

The characterization of SPNs is a challenging issue for chest radiologists. It is important, however, because these nodules have a 30–40% chance of being malignant.[7,8] Morphological evaluation of CT findings is useful for differentiation between benign and malignant nodules when typical benign or malignant features are present, but there is a considerable overlap between CT characteristics.[9] Various strategies other than simple morphologic evaluations have been developed for the differentiation of malignant and benign nodules. The most interesting of these is hemodynamic evaluation of SPN using time-resolved contrast-enhanced CT imaging, which has shown excellent diagnostic efficacy.[10]

PET/CT, with its metabolic data of ^{18}F-FDG cellular uptake in addition to morphologic CT data, has also been applied for SPN characterization with promising results. In a study by Yi et al,[11] PET/CT proved to be better in terms of malignant nodule characterization by providing higher sensitivity and accuracy than the use of helical dynamic CT. That study suggested that PET/CT may be performed as the first-line evaluation tool for SPN characterization. SPNs demonstrating high ^{18}F-FDG uptake should be considered malignant, although false-positive results can be seen in inflammatory or infectious lesions such as rheumatoid nodules, active tuberculosis, and histoplasmosis.[12,13] Thus, some researchers insist PET/CT should be selectively performed to characterize SPNs that show indeterminate results at dynamic helical CT.[7]

The high specificity of ^{18}F-FDG PET for the diagnosis of benign lesions serves an important role in diagnostic performance. SPNs with low ^{18}F-FDG uptake may be considered benign, albeit some malignancies are known to demonstrate low avidity for ^{18}F-FDG, including adenocarcinoma in situ (AIS), minimally invasive adenocarcinoma (MIA), adenocarcinomas with a lepidic-growth predominant subtype, solitary nodular mucinous adenocarcinoma, small malignant pulmonary nodules of $<$10 mm in diameter, and carcinoids.[1,14–18] This renders ^{18}F-FDG PET unreliable in some situations, as demonstrated by Kim et al,[19] who reported that 75% (40 of 53 nodules) of pure ground-glass nodules (GGNs) are histologically diagnosed as AIS or adenocarcinoma, with a predominant lepidic-growth pattern. Importantly, in their study all 24 patients with proven malignancy and GGNs, in whom PET was performed, showed negative results.

In a comparative study of PET/CT and PET alone or CT alone for the characterization of SPNs performed by Jeong et al,[20] PET/CT was superior, with a specificity of 77%; PET alone and CT alone showed specificities of 71% and 66%, respectively. PET/CT demonstrated significantly higher areas under the curve (Az) values in receiver operating characteristics (ROC) analysis, and greater interobserver agreement than those acquired for PET alone and CT alone. These results suggest that by providing metabolic PET data, the use of PET/CT allows more confidence and consistency in the characterization of SPNs than the use of CT alone.

Volume-Based Assessment of PET/CT in Lung Cancer

Although tumor-node-metastasis (TNM) staging serves as a standard reference in the decision of treatment option, it is apparent that it lacks correlation with the biological behavior of the tumor. Thus, identification and development of additional prognostic biomarkers have been widely studied.

As ^{18}F-FDG PET/CT imaging has become an essential tool for staging in nonsmall-cell lung cancer (NSCLC) patients, metabolic parameters have been studied as potential imaging biomarkers. The standardized uptake value (SUV), a semiquantitative index for ^{18}F-FDG tumor uptake in PET, is increasingly accepted as a promising biomarker of patient outcome and a surrogate marker for tumor aggressiveness.[4,21,22] However, it still remains uncertain whether SUV is a reliable independent prognostic factor and whether it can provide additional prognostic information to TNM stage [23,24]. A widely used single value measurement of tumor SUV, such as maximum standardized uptake value (SUVmax), has its own limitation due to heterogeneous tumor uptake.

Recently, the volume-based parameters of ^{18}F-FDG PET, 3D measurements of total tumor metabolic activity, have been reported to be a significant prognostic factor for clinical outcome in patients with various solid tumors.[4,25–28] In contrast to SUVmax, these parameters incorporate both metabolic activity and 3D tumor volume, allowing a more accurate assessment of real tumor burden. Due to the variable shape of tumors, unidimensional measurement of tumor size such as largest tumor diameter, used in TNM staging system or the Response Evaluation Criteria in Solid Tumors (RECIST) system, often cannot accurately represent the real tumor burden.

Studies using these parameters for NSCLC patients showed promising results. Hyun et al[4,25] reported that metabolic tumor volume (MTV) and total lesion glycolysis (TLG) are significantly associated with an increased risk of

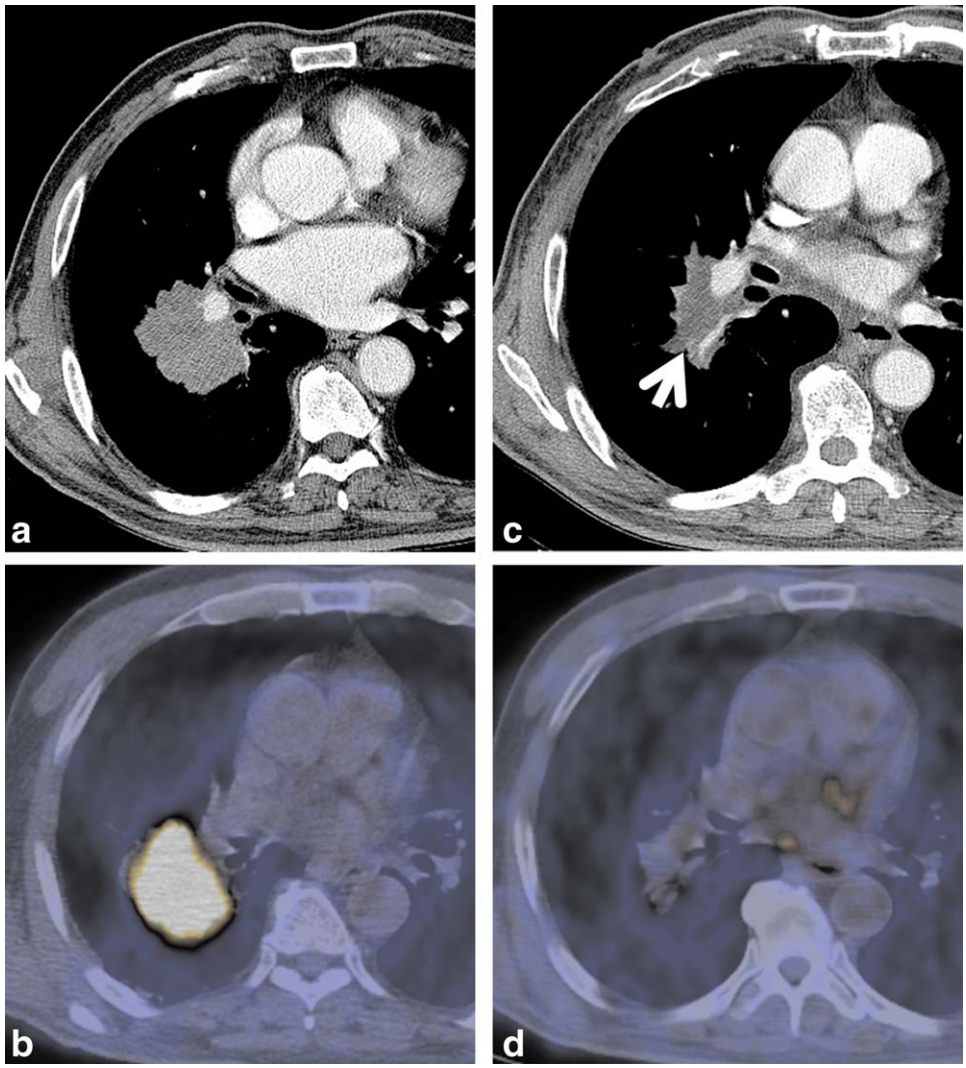

FIGURE 1: PET response evaluation after neoadjuvant therapy in a 68-year-old man with N2 squamous cell carcinoma of the lung. Patient had positive nodes at subcarinal area (N2 disease). A,B: Mediastinal window of CT (A) and PET (B) scans before neoadjuvant therapy show a 5.8-cm size mass in superior segment of right lower lobe with high glucose uptake (SUVmax, 11.2). C,D: Follow-up CT scan (C) demonstrates remaining tumor (arrow), but PET scan (D) shows no residual tumor at initial tumor site. When surgery was performed, no remaining tumor was detected on histopathologic examination.

recurrence and death, with a better predictive performance than SUVmax in early-stage (stage I and II) and stage IIIA NSCLC patients. These studies suggested that a new prognostic stratification based on volume-base PET parameters and TNM stage may help identify appropriate patients for risk-adapted treatment strategies and prospective clinical trials.

PET/CT as a Follow-up Imaging Tool

The accurate follow-up assessment of response to treatment of malignant lesions managed with radiotherapy or chemotherapy is a crucial part of tumor evaluation. Serial CT measurements of tumor dimension and consequent categorization according to World Health Organization (WHO) criteria provide information on prognosis, and may determine the need for further treatment.[29] However, there are several well-established limitations for treatment response evaluation in NSCLC patients, such as tumors obscured by atelectasis or radiation pneumonitis, and false-negative or false-positive lymph nodes.[30] Functional data acquired by ^{18}F-FDG PET can aid in more accurate early response evaluation.

In a comparison study on the prognostic value of early posttreatment FDG-PET and CT scanning in NSCLC patients treated with radical radiotherapy, posttreatment PET response was a better predictor of survival than CT response[31] (Fig. 1). The number of complete responders on PET was significantly higher than that on CT, which will have an impact on management and costs of treatment.

Standardizing response assessment for PET in treatment monitoring is another crucial issue for tumor evaluation. Recently, PET Response Criteria in Solid Tumors (PERCIST 1.0) were proposed.[32] In PERCIST, response to

therapy is assessed as the percentage reduction in peak SUL (SUV corrected for lean body mass, SUV_{lbm}) between the pre- and posttreatment scans.[32] Many aspects of PERCIST 1.0 are still controversial but the criteria are intended to represent a foundation for validating quantitative approaches to monitoring PET tumor response.

There is still controversy over the optimal follow-up timepoint and the issue of radiation exposure to patients, with an effective dose per PET/CT as high as 25 mSv.[33] The use of routine follow-up PET/CT in patients other than those postradiotherapy or chemotherapy is therefore not commonplace.

MRI in Lung Cancer

Proton MRI was the latest modality to be introduced into lung imaging practice. Acceptance in the lung imaging community is growing constantly, but introduction is slowed by the fact that MRI is perceived to be more complex than other modalities. Push-button protocols haven been made available by different vendors, and the start has been made easy.[34,35] Nevertheless, thoracic radiologists trained in x-ray and CT often feel uncomfortable with the different contrast, lower spatial resolution, and image artifacts of MRI.[36] The value of MRI to replace x-ray and CT, when radiation exposure or administration of iodinated contrast material would be contraindicated, is well acknowledged: ie, for pediatric patients and pregnant women or for scientific use. MRI combines morphologic and functional imaging aspects in a single examination and might challenge even molecular imaging techniques in the near future. It also serves in difficult clinical problems encountered in daily routine, such as assessment of the mediastinum and chest wall. In the context of lung cancer staging, MRI contributes to all aspects of the TNM staging system.

Available Protocols

The marketing terminology used by different vendors makes it difficult for new users to select appropriate protocols and to customize them to their needs. A summary of the currently available techniques with protocol suggestions for different clinical questions together with a list of acronyms allowing for "translation" of the protocols into different vendor platforms may be considered helpful for a start.[35,37,38] The core protocol for detection of pulmonary nodules and lung cancer imaging comprises 1) T_2-weighted fast spin echo sequences (FSE), optional with partial Fourier acquisition in coronal and transverse orientation (aiming at infiltrates and soft parenchymal lesions); 2) T_2-weighted fast spin echo sequences (FSE) with inversion recovery pulse or spectral suppression of fat signal (aiming at lymph nodes and bone lesions); 3) steady-state free precession (SSFP) images in coronal or transverse orientation (aiming at respiratory motion and lung vasculature); 4) T_1-weighted 3D gradient echo sequences (3D-GRE) with volumetric interpolation in coronal or transverse orientation and including pre- and postintravenous injection of contrast material (aiming at nodules and masses). Optional sequences comprise 5) dynamic contrast-enhanced (DCE) imaging of the whole lung or focused on lung lesions, preferentially as time-resolved 3D-GRE (aiming at lung perfusion), and 6) diffusion-weighted imaging (DWI) with fat signal suppression (aiming at lymph nodes and for lesion characterization).

The protocols are basically intended for fast (multi-) breath-hold scanning with in-room times between 15 and 30 minutes.[39] For basic diagnosis, noncontrast-enhanced series are considered sufficient (~15 min in-room time). For lung cancer staging, contrast-enhanced series to detect tumor necrosis and pleural involvement is strongly recommended (adds 5 min). The optional extensions to the protocol with dynamic contrast-enhanced MRI and visualization of respiratory motion contribute functional information and can be acquired within an additional 5–15 minutes, which finally makes up ~30 minutes for the "have it all" examination. These protocol suggestions can be transferred from 1.5 to 3.0T MR scanners.[40] The main motivation for the transition from 1.5 to 3.0T MRI system is the improved signal-to-noise ratio (SNR), which may lead to a potentially higher contrast and clearer delineation between normal lung parenchyma and solid nodules in lung imaging.[41] Theoretically, however, problems related with the increase in field strength such as more pronounced susceptibility artifacts and dielectric effects may result in unfavorable results.[42] Recent studies on lung MRI with 3.0T scanners showed profit from a higher lesion-to-background contrast, particularly in 3D-GRE sequences, but significantly increased susceptibility artifacts, particularly in steady-state GRE sequences.[40,43,44] In an experimental study reported by Regier et al,[42] detection rates of 3D-GRE and half-Fourier FSE sequences at 3.0T for lung nodules greater than 5 mm in diameter were comparable to standard and low-dose CT and 1.5T MRI as well. In a recently published observer preference study, the imaging characteristics of different pulse sequences used for lung MRI did not substantially differ between 1.5 and 3.0T.[40] Overall, transfer of the concept to 3.0T results in acceptable or even positive changes for most sequence types. Moreover, a large number of variations of these sequences and many experimental sequences have been published, but have not yet arrived in clinical routine.

MRI for the Detection of Pulmonary Nodules

The detection of small solid or soft tissue lesions ("nodules") is a key clinical question. The sensitivity of MRI for lung nodules larger than 4 mm in diameter ranges between 80 and 90% and reaches 100% for lesions larger than 8 mm in diameter.[45] Depending on the sequence technique and the signal intensity of the lesions and given

optimum conditions (breath-hold or adequate gating/triggering), a threshold size of 3–4 mm can be assumed for lung nodule detection with MRI.[42,46–48] For DWI alone, Regier et al[49] found a sensitivity of 43.8% for lung nodules of 5 mm in diameter, which increased to 97% at 10 mm (threshold size around 6 mm). Koyama et al[50] demonstrated a lower nodule detection rate with DWI compared to a short TI inversion recovery (STIR) sequence. From the readers' point of view, it might be even faster and more efficient to read lung MRI for pulmonary nodules than CT, since the nodules appear with bright signal against the dark background of the healthy lung tissue.[40] Calcified nodules tend to disappear in the background, as they have no inherent signal, whereas contrast-filled vascular lesions will be highly visible on T_1-weighted images.[51] In particular for the detection of malignant lesions with high perfusion and intense enhancement, the intravenous administration of paramagnetic contrast material might be helpful and even increase detection rates.[52]

MRI for the Assessment of Malignancy and Tumor Viability

The first attempts to differentiate among tumor, necrosis, and atelectatic lung by T_1- and T_2-relaxation times date back to 1988, when Shioya et al[53] detected a large overlap for all three situations. Malignant primary lung lesions, carcinoma, metastases, carcinoid and lymphoma usually show a nonspecific low or intermediate signal intensity on T_1-weighted images and a high signal intensity on T_2-weighted images.[46,54] Criteria for the characterization of mucinous tumors and hamartomas on T_1- and T_2-weighted images have been described,[55,56] but the differentiation between malignant and benign lesions with morphologic sequences remains unsatisfactory. Only recently, Koyama et al[50] used a STIR sequence and achieved a sensitivity of 83.3% and a specificity of 60.6% for detecting lung adenocarcinoma nodules.

The diagnostic accuracy of DWI for benign/malignant discrimination of pulmonary nodules has been discussed intensively and was addressed by a number of studies. Studies have shown that sensitivity between 70% and 89% and specificity of 61–97% can be achieved with various b-values.[75–77] Razek et al[57] showed a lower apparent diffusion coefficient (ADC) value of lung cancer being associated with higher pathological tumor grade and metastatic lymph nodes. However, most results were obtained in relatively small populations with high pretest probabilities and often do not reflect the problem of false-positive findings, since granuloma and fibrous lesions may well appear with the same signal intensity as malignant lesions on DWI. A meta-analysis of 10 studies including 545 patients revealed a pooled sensitivity of 0.84 and a pooled specificity of 0.84 for DWI of malignant pulmonary lesions.[58] In patients with high pretest probabilities, DWI enabled confirmation of malignant pulmonary lesions. In patients with low pretest probabilities, DWI enabled exclusion of malignant pulmonary lesion. Wu et al[59] concluded that further high-quality prospective studies are needed before DWI can be recommended to differentiate malignant from benign pulmonary lesions. Another potential important role for DWI is the evaluation of early response to systemic treatment. Several studies demonstrated that an increase in ADC correlates with a response to treatment,[60–62] while ADC values obtained at 1.5 and 3.0T correlate well.[63]

DCE MRI is another intensively studied approach for the differentiation of malignant and benign lesions[64–66] (Fig. 2). The available data achieved specificities of 52–96% and sensitivities of 54–100% with diagnostic accuracies of 75–94%. In some studies, DCE MRI even matched the accuracies of contrast-enhanced MDCT and FDG PET/CT.[64] These positive predictive data as achieved in small, high-prevalence populations are disputable. On the contrary, just as in dynamic CT, it can be assumed that DCE MRI of solid pulmonary lesions has a high negative predictive value in cases of very low or missing enhancement after intravenous contrast application.[67] The use of DCE MRI to monitor response in systemic treatment has been studied as well.[68] Decreased tumor size correlated well with decreased values of all MR-derived pharmacokinetic parameters (K [trans]) histogram, K [ep] histogram). A potential value of DCE for the differentiation of lung cancer subtypes has been demonstrated by Pauls et al[69] in 68 lung cancer patients.

Both DWI and DCE MRI cannot yet be considered robust, highly standardized, and simple techniques for clinical use. The applied protocols vary widely and solutions for basic problems such as compensation for respiratory motion and for the nonlinearity of blood/tissue-signal with gadolinium-concentration are still subject to research [59,70]. Further methods to evaluate tumor viability based on multiparametric MRI are on an early, experimental level [71].

Implementation of Lung MRI Into Hybrid Systems

In comparison to PET/CT, PET/MRI promises to contribute additional information due to its higher soft-tissue contrast and a significant reduction of radiation exposure [72]. For staging of metastatic cancer in 40 consecutive patients, Stolzmann et al [73] implemented a 3D Dixon-based, dual-echo GRE pulse sequence on a hybrid 3.0T PET/MRI system. MRI of the hybrid system detected fewer nodules than low-dose CT (58% instead of 66%) but was almost equally diagnostic in detecting patients with metastases (83% instead of 85%). Thus, 3D GRE sequences may be a suitable approach in clinical whole-body (WB) PET/MRI examinations. Schmidt et al[74] showed the diagnostic image quality of simultaneous lung MRI with DWI and PET in

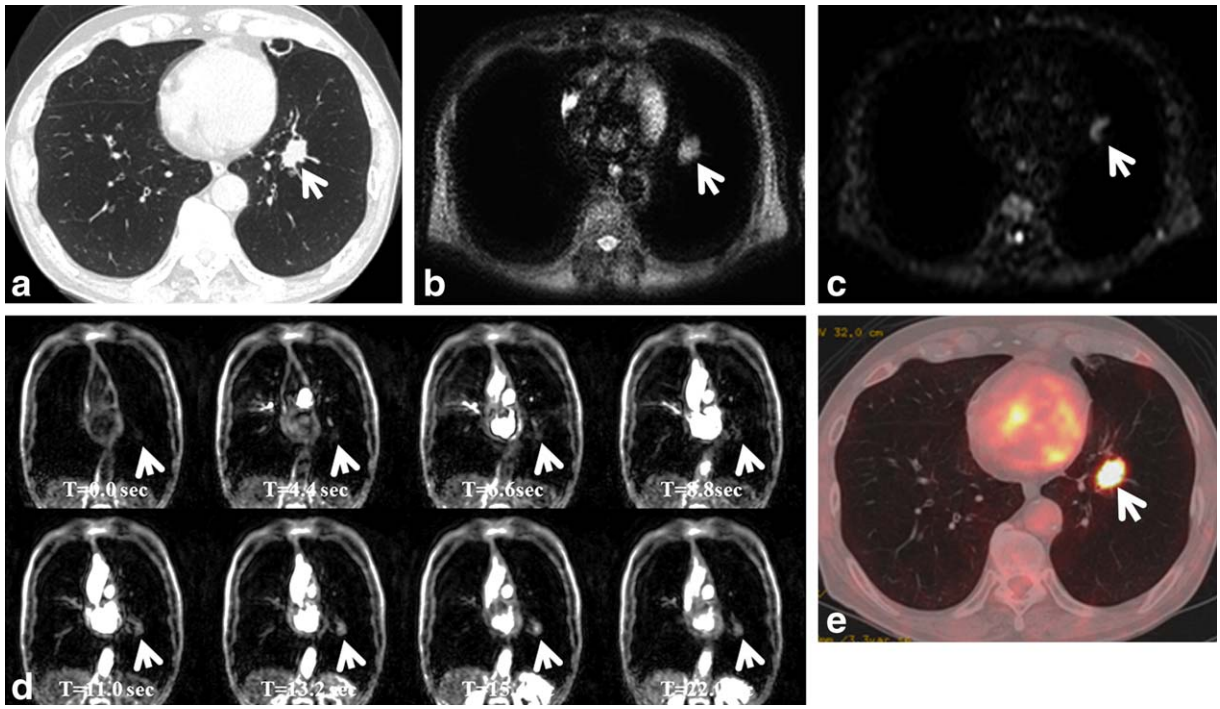

FIGURE 2: MRI depiction of lung adenocarcinoma in a 75-year-old man. A: Lung window image of thin-section (1.5-mm section thickness) CT scan obtained at ventricular level shows a nodule of 18 mm in diameter (arrow) in the left lower lobe with pulmonary emphysema in both lungs. B: STIR turbo spin-echo imaging shows a high-intensity nodule (arrow) in the left lung. C: Diffusion-weighted MR image manifests the nodule (arrow) as high-signal intensity lesion, suggesting a malignant one. D: Dynamic MRI with ultrafast-gradient-echo technique (left to right: upper line, t = 0.0 sec; t = 4.4 sec; t = 6.6 sec; and lower line, t = 11.0 sec; t = 13.2 sec; t = 15.4 sec, and t = 22.0 sec) shows a well-enhancing nodule (arrow) in the left lower lung zone, and heterogeneous enhancement in both lungs due to pulmonary emphysema. The nodule exhibits high enhancement in the systemic circulation phase (t = 11.0–22.0 sec) owing to high blood supply from systemic circulation. This nodule was assessed as a malignant lesion on dynamic contrast-enhanced MRI. E: PET/CT demonstrates high FDG-uptakes within the nodule (arrow).

15 patients with lung tumors using a hybrid system. Image quality of the PET component was equal compared to a PET/CT scanner. The minimum ADC and maximum SUV as measures of the cell density and glucose metabolism showed a significant reverse correlation ($r = –0.80$; $P = 0.0006$), suggesting that both parameters can be quantitatively assessed with the hybrid system and be used for tissue characterization. In a small study, Chandarana et al[75] demonstrated higher sensitivity of PET/MRI (70.3% for all nodules, 95.6% for FDG-avid nodules, and 88.6% for nodules >0.5 cm) as compared with PET and MRI alone, while the sensitivity for small (<0.5 cm) non-FDG-avid nodules was very low.

While the application of hybrid PET/MRI in the lung will require further investigation, it is anticipated that in particular M-staging of lung cancer shall benefit from a hybrid approach (Fig. 3). MRI is known to be of higher accuracy than PET/CT when assessing brain, liver, and bones for distant metastases.[76,77] Less impact can be anticipated for nodal staging, since nodal staging with both MRI and CT is size-based.[78] However, in addition to morphology, it is anticipated that novel radiotracers will allow for improvement in molecular and functional tumor assessment to incorporate biological properties, which will facilitate more targeted therapy. Moreover, the potential value of 4D MRI for motion correction of PET opens interesting perspectives, since 4D CT for motion correction appears prohibitive regarding radiation exposure.[79,80]

MRI as a Potential Tool for Early Detection of Lung Cancer

The prognosis of lung cancer increases significantly with detection in the early stages, hence early detection programs in high-risk patients have been advocated.[81,82] Among a number of national and international initiatives, the first study to demonstrate a 20% reduced lung cancer mortality in smokers was the national lung screening trial.[83] However, there is a trade-off, with an anticipated radiation-induced additional cancer risk of 0.5–5.5% in active or past smokers if screened yearly between 50 and 75 years.[84] Therefore, an MRI-based early detection study might be very attractive.

From a technical point of view, lung MRI can be considered a potentially effective screening tool. The benchmark sensitivity to be met for an effective lung cancer early detection program has been calculated as >75%.[82] This seems to be easy with the above-mentioned nodule detection rates for

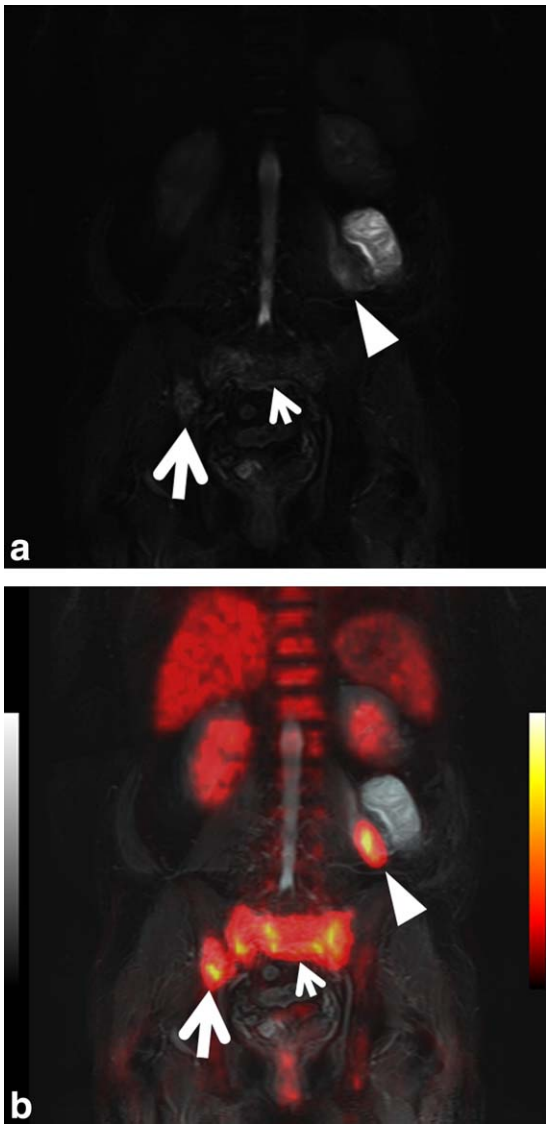

FIGURE 3: Lung cancer accompanying right iliac and sacral bone and psoas muscle metastases in a 75-year-old male. A: Whole-body STIR turbo spin-echo image shows metastatic bone and soft-tissue lesions as high-signal intensity abnormalities in right ilium (arrow), sacrum (small arrow), and in psoas muscle (arrowhead). In addition to psoas muscle metastasis, high-signal intensity mass is observed in the abdomen, which proved to be a neurogenic tumor with histological examination of biopsy specimen. B: Hybrid whole-body PET and STIR turbo spin-echo (MRI/PET) image shows right iliac (arrow) and sacral (small arrow) bone metastases and psoas muscle metastasis (arrowhead) as high FDG-uptake lesions. The mass adjacent to psoas muscle lesion shows little FDG uptake, suggesting the benign nature of the lesion.

MRI. Wu et al[52] retrospectively evaluated WB MRI of 11,766 asymptomatic individuals who enrolled for a commercial WB screening MRI program. The chest part comprised half Fourier FSE and 3D-GRE images; 4.8% had suspicious lung nodules including a total of 49 primary lung cancers (0.4%). For smokers aged 51 to 70 years, the detection rate was 1.4%. TNM stage I disease accounted for 37 (75.5%). The mean size of detected lung cancers was 1.98 cm (median, 1.5 cm; range, 0.5–8.2 cm). The most histological types were adenocarcinoma in 38 (77.6%). These results are well in line with CT screening programs.

Sommer et al[82] conducted their study in a subset with a 20% prevalence of malignancy and achieved a sensitivity of 78%, a specificity of 88%, a positive predictive value of 87%, and a negative predictive value of 51%. The false-positive rate of only 5% appeared very attractive if compared to the 23.3% false-positive findings in the first round of the National Lung Screening Trial (NLST). This indicates a potentially very interesting role for MRI as an adjunct to CT-based lung cancer screening studies in the evaluation of suspicious findings. An additional MRI scan in all patients with positive findings in the first screening round could help to reduce the number of cases scheduled for further diagnostic procedures.

However, cost-effectiveness and the final impact of an MRI-based lung cancer screening trial on lung cancer mortality are subject to discussion. Therefore, a broad application of lung MRI for early lung cancer detection outside clinical studies cannot be recommended, and further study will be required once all ongoing screening trial results are available.

PET/CT Versus MRI in Lung Cancer Staging

Accurate staging of patients with NSCLC provides important prognostic information with regard to survival. Currently, lung cancer staging is based on the TNM classification, which has been revised recently.[85] The proposed changes in this recent revision were aimed at improving correlation between tumors and prognosis.

Staging of lung cancer also guides the clinical decision with regard to the selection of optimal treatment modality. In general, patients with stage IIIB disease are considered inappropriate for surgery, even though practice guidelines vary among centers.[86] Stage I and II patients are preferably treated by complete resection, with some receiving additional adjuvant chemotherapy.[87] Stage IIIA lung cancer represents a relatively heterogeneous group of patients with a wider range of presentation, resulting in a greater variety of multimodal therapeutic approaches, and controversy for optimal therapy for those patients still remains.[86]

The evidence of the role of PET/CT in this context will be reviewed with comparison to those of the individual CT and PET components. In addition, the role of MRI will also be reviewed.

TUMOR STAGING. Similar to solitary nodule diagnosis, combined PET/CT is superior to CT or PET alone in primary tumor staging.[88–93] Thus, PET/CT is better able to differentiate tumor tissue from postobstructive atelectasis,[6] while it also allows for a more precise delineation of the

primary tumor location, chest-wall infiltration, and mediastinal invasion by the tumor.[8,91] Antoch et al[6] reported that the primary tumor stage is correctly determined in more patients with PET/CT than with CT alone. Of the 16 patients in whom the T stage was verified histopathologically, the T stage could be accurately determined with PET/CT in 15 (15 of 16, 93.8%) patients and CT enabled accurate staging in 12 (12 of 16, 75%) patients.

Halpern et al[88] demonstrated a tumor staging accuracy rate of 97% with PET/CT compared with 67% with PET only. This superiority was mainly attributed to the CT component of the integrated imaging. Lardinois et al[90] reported that PET/CT provides additional information with respect to tumor stage in 13 of 40 patients (32.5%) as compared with visual correlation of PET and CT. These included precise evaluation of mediastinal invasion in three patients and of chest-wall infiltration in three patients, and correct differentiation between tumor and peritumoral inflammation or atelectasis in seven patients. In addition, the accuracy of tumor staging was significantly more accurate with PET/CT than with CT alone, PET alone, or visual correlation of PET and CT.

One important point in T staging is that PET alone has a limited role in dry pleural dissemination (stage M1a disease)[89] and this can cause failed thoracotomy procedures. Shim et al[92] evaluated PET/CT of 172 lung adenocarcinoma patients (eight with dry pleural dissemination and 164 without) for findings of dry pleural dissemination. With PET only, the sensitivity, specificity, and accuracy of dry pleural dissemination were 25%, 90%, and 87%, respectively; by PET plus CT these were all 100%, demonstrating the vital importance of the CT findings of dry pleural dissemination: multiple small pleural nodules and uneven pleural thickening.

The classical indication for thoracic MRI in lung cancer is the determination of chest wall or mediastinal invasion, in particular, for superior sulcus (Pancoast) tumors using the excellent soft-tissue contrast.[78,94] Limited data exist regarding direct comparison of MRI with CT or PET/CT for diagnostic performance of T stage assessment, but a recent study reported WB PET/MR is more accurate in terms of T staging compared with that of PET/CT, which is possible because morphologic thoracic MRI information allows better delineation of tumor size and better detection of mediastinal tumor extent than information from CT component of PET/CT.[95]

NODAL STAGING. CT has low efficacy in the evaluation of mediastinal nodal metastasis in NSCLC patients.[6,88,93] In spite of advances in CT technology, the accuracy for mediastinal staging has not improved over the past decade.[3] This is inherently caused by the criterion of nodal size, with up to 21% of nodes 10 mm or smaller being malignant, while up to 40% of those larger than 10 mm are benign.[96]

PET is substantially more sensitive and specific in the detection and characterization of metastases to mediastinal lymph nodes[3,6,8,88,97] (Fig. 4). This improved sensitivity is due to its ability to detect metabolic activity in small metastatic lymph nodes, and it has been suggested that eligible patients with negative mediastinal nodes on PET may proceed directly to thoracotomy without additional mediastinoscopy.[8,98] However, several factors can affect the accuracy of SUV measurement; these include blood glucose level, patient weight, partial-volume averaging effect, and recovery coefficient.[93] In addition, increased FDG uptake in a benign node can be caused by active inflammation or reactive hyperplasia, which may be indistinguishable from malignancy. Therefore, it is difficult to differentiate between benign and malignant lymph nodes with morphologic or metabolic data alone.

To pinpoint mediastinal lesions, PET images must be correlated with CT images. Several early approaches using software fusion of images obtained by CT and PET from separate scanners showed no significant increase in the accuracy of mediastinal staging over that obtained by PET alone.[88,99–101] However, it has been suggested that the advantages of integrated data of PET/CT to disclose the exact anatomic location may be of benefit for differentiating N1 from N2 disease and mediastinal blood pool from nodal uptake.[88]

Lardinois et al[90] compared N-staging accuracy of PET/CT, PET alone, and visual correlation of PET and CT by means of comparing scores ranging from 0 to 3. In this study, the scores were determined by correlating with the standard reference obtained through histopathologic assessment. They reported significantly more accurate nodal staging with integrated PET/CT than with PET alone or with visual correlation of PET and CT in NSCLC patients.

Shim et al,[93] in their comparative study of integrated PET/CT and stand-alone CT for lung cancer staging, showed PET/CT to be superior for nodal staging. The sensitivity, specificity, and accuracy of CT for malignant nodes were 70%, 69%, and 69%, respectively, whereas those of PET/CT were 85%, 84%, and 84%.

Metastasis to supraclavicular lymph nodes (N3 disease) in lung cancer is an indicator of inoperable disease.[85] In a comparative study of PET/CT versus CT alone for nonpalpable lymph node metastases in lung cancer patients, PET/CT and CT showed similar sensitivity (92%) and negative predictive value (93%).[102] However, PET/CT was helpful in cases with extensive beam-hardening artifact caused by contrast medium in the adjacent subclavian vein.

In the morphologic MRI protocols, the differentiation of malignant and benign lesions basically relies on the same criterion as in CT, which is size of the node.[103] DWI, as

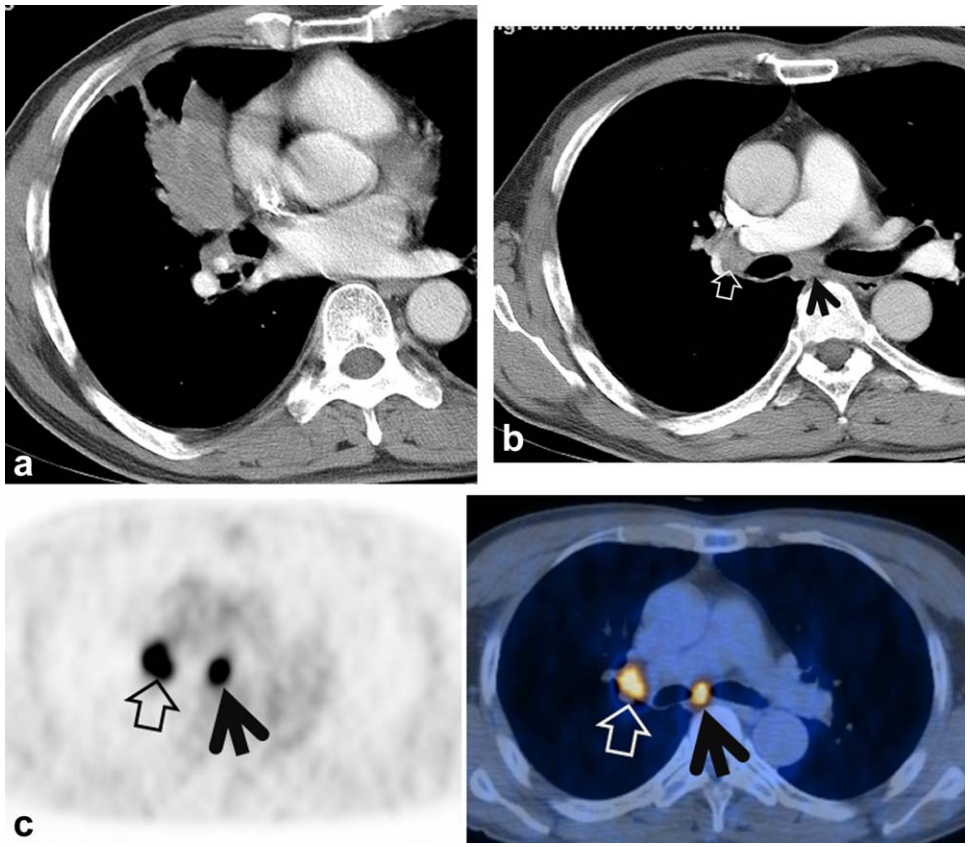

FIGURE 4: True metastatic nodes harboring cancer cells in right hilar (station 10R) and subcarinal (station 7) regions observed at PET/CT in a 67-year-old man with lung adenocarcinoma. A: Mediastinal window of CT scan (5.0-mm section thickness) obtained at inferior pulmonary vein level shows a 6.5-cm size mass in right middle lobe. B: Enhanced CT scan obtained at distal main bronchial level demonstrates enlarged lymph nodes in subcarinal (arrow, 11 mm in short-axis diameter) and right hilar (open arrow, 12 mm in short-axis diameter) regions. C: PET (left) and PET/CT (right) images disclose high glucose uptake at subcarinal (arrows) and right hilar (open arrows) nodes.

recommended for WB staging of lung cancer, also covers mediastinal metastases, but a clear advantage of DWI over other MRI protocols has not been confirmed so far.[104,105] In comparison to PET, some studies suggest a similar sensitivity but lower false-positive rates for N staging of NSCLC with DWI.[106] In 160 lung cancers, Usuda et al[107] found 144 correctly N-staged cases with DWI and 133 with PET/CT, with both modalities having a tendency to understage. In that study, sensitivity, accuracy, and negative predictive value for N staging by DWI were significantly higher than those by PET/CT. A recent meta-analysis by Wu et al,[108] based on 19 studies with a total of 2845 pathologically proven cases, confirmed an equal pooled sensitivity of DWI (0.72) compared to PET/CT (0.75; $P = 0.09$). The pooled specificity estimate for DWI (0.95) was significantly greater than for FDG PET/CT (0.89; $P = 0.02$).

Another, more fundamental MR sequence, short TI inversion recovery (STIR) turbo spin-echo (SE), has been suggested as being more useful than CT, PET/CT, or DWI.[58,109–111] A recently published article, which directly compared the diagnostic performance of N stage assessment among STIR turbo SE imaging, DWI, and PET/CT, demonstrated that sensitivity or accuracy of STIR turbo SE imaging (quantitative sensitivity: 82.8%, qualitative sensitivity: 77.4%, quantitative accuracy: 86.8%) proved to be significantly higher than those of DWI (74.2%, 71.0% and 84.4%, respectively) and FDG-PET/CT (quantitative sensitivity: 74.2%).[111] These results suggest that STIR turbo SE imaging may be the preferred MR technique prior to surgical treatment or lymph node sampling, during thoracotomy or mediastinoscopy for accurate pathologic TNM staging, or before chemotherapy/radiation therapy (Fig. 5).[111]

METASTASIS STAGING. For M staging, an important role for functional PET data is the detection of occult metastases. Unknown metastases are detected on PET in 3–24% of the patients with negative results on conventional staging workup[2,112–114] (Fig. 6). The detection rate may vary partially depending on the "definition" of conventional staging in their study.

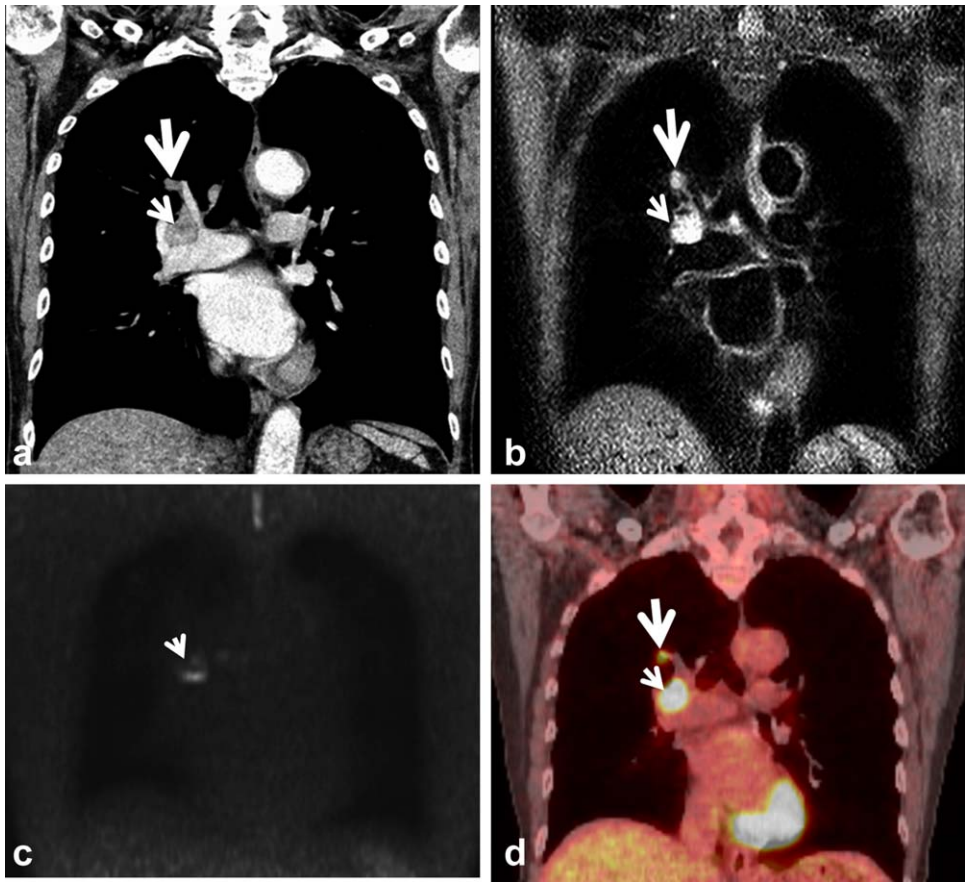

FIGURE 5: Lung adenocarcinoma and ipsilateral hilar nodal metastasis (N1 stage) in a 65-year-old man. A: Thin-section, contrast-enhanced, and coronal reformatted image shows primary lesion (large arrow) and right hilar lymph node enlargement (arrow). Short-axis diameter of this lymph node is 13 mm, and was regarded as a malignant node (N1 disease). B: STIR turbo spin-echo image demonstrates primary lesion (large arrow) and lymph node metastasis (arrow) as high-signal intensity lesions than chest wall muscle, suggesting that both lesions contain malignant tumor cells. C: On diffusion-weighted MR image, the node (arrow) persistently appears as high-signal intensity lesion with primary tumor signal disappeared. The node proved to be malignant on surgery (N1 disease). D: PET/CT demonstrates primary lesion (large arrow) and lymph node (arrow) with both having high FDG uptake, indicating both lesions contain cancer cells.

Stroobants et al[114] evaluated the additional value of WB PET in the distant staging of NSCLC, including 144 patients in whom conventional staging was negative or equivocal for metastases, and who underwent WB PET as part of their initial work-up. Conventional staging was defined as chest CT, abdominal ultrasound or CT, and bone scintigraphy or brain CT on indication. Additional lesions suspected for metastases were found on WB PET in 11 patients and were true-positive in seven (7 of 144, 4.9%) patients.

As important as the detection of occult metastatic spread, another important role for functional PET data of ^{18}F-FDG PET-CT is to correctly exclude metastatic involvement in 3–19% of the patients with suspicious lesions on conventional staging.[2,8,91,112,113] In lesions less than 1 cm in diameter, however, exclusion of metastatic disease remains problematic, with up to 20% of micrometastatic disease missed by PET/CT.[2]

Occasionally, the significance of isolated areas of avid FDG uptake at PET is uncertain without an anatomical reference image.[8] Morphologic CT data of PET/CT offers advantages for accurate anatomical localization, which usually resolves this matter (Fig. 6).

The predominant role of MRI for M staging is the detection of brain metastases. Approaches for staging of distant metastases in extrathoracic organs by using WB MRI will be discussed below. However, it should be mentioned that the standard protocols for lung MRI in cancer staging recommend including the upper abdomen and the complete chest wall into the volume to avoid missing metastatic spread to the adrenal glands and spine.

Performance Comparison in Cancer Staging Between PET/CT and WB MRI

WB MRI has become feasible for fast imaging and can be used for staging of malignant conditions.[115–117] Yi et al [118]

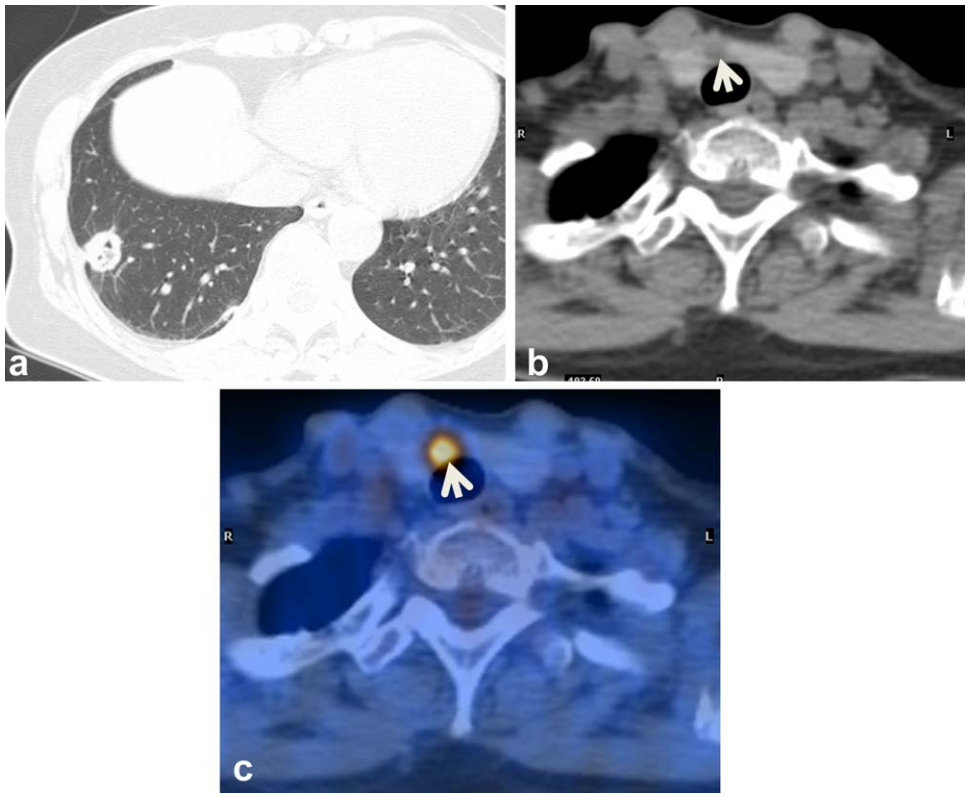

FIGURE 6: Unexpected cancer detection at PET/CT in a 61-year-old woman who has lung cancer in right lower lobe. A: Lung window of CT scan (5.0-mm section thickness) obtained at liver dome shows a 22-mm size malignant-morphology nodule in right lower lobe which proved to be lung adenocarcinoma. B: CT component image of PET/CT demonstrates a 12-mm size low-attenuation nodule (arrow) in right thyroid gland. C: PET-CT image discloses high glucose uptake within the nodule, which proved to be papillary thyroid carcinoma (PTC).

reported similar accuracy in a prospective study comparing PET/CT and 3.0T unenhanced WB MRI in NSCLC. For M stage determination, even though the differences were not statistically significant, WB MRI was more useful for detection of brain and hepatic metastases, whereas PET/CT was more useful for detection of lymph node and soft-tissue metastases. The advantages for detection of brain and hepatic metastases in MRI can be attributed to the better contrast on MR images and physiologic FDG uptake in these organs which may have obscured their presence on PET/CT.

Recently, a study comparing the clinical effectiveness of coregistered WB PET/MRI and WB PET/CT plus dedicated brain MRI in patients with resectable NSCLC was reported.[95] PET/MRI demonstrated an incremental difference of 4.2% in correct upstaging, which was similar to the performance of PET/CT plus dedicated brain MRI. Conversely, WB PET/MRI was more accurate and demonstrated less understaging than PET/CT plus brain MRI (12.6% vs. 23.3%, respectively).

Conclusion

CT is the workhorse for lung cancer diagnosis, and integrated PET/CT currently has the upper hand for staging of lung cancer. However, both MRI as a sole test and PET/MRI for future evaluation of lung cancer patients already have a role to play. It is anticipated that this role will grow and novel therapies will become available.

References

1. Lowe VJ, Fletcher JW, Gobar L, et al. Prospective investigation of positron emission tomography in lung nodules. J Clin Oncol 1998;16: 1075–1084.
2. Stroobants S, Verschakelen J, Vansteenkiste J. Value of FDG-PET in the management of non-small cell lung cancer. Eur J Radiol 2003;45: 49–59.
3. Toloza EM, Harpole L, McCrory DC. Noninvasive staging of non-small cell lung cancer: a review of the current evidence. Chest 2003;123: 137S–146S.
4. Hyun SH, Choi JY, Kim K, et al. Volume-based parameters of (18)F-fluorodeoxyglucose positron emission tomography/computed tomography improve outcome prediction in early-stage non-small cell lung cancer after surgical resection. Ann Surg 2013;257:364–370.
5. Beyer T, Townsend DW, Brun T, et al. A combined PET/CT scanner for clinical oncology. J Nucl Med 2000;41:1369–1379.
6. Antoch G, Stattaus J, Nemat AT, et al. Non-small cell lung cancer: dual-modality PET/CT in preoperative staging. Radiology 2003;229: 526–533.
7. Jeong YJ, Yi CA, Lee KS. Solitary pulmonary nodules: detection, characterization, and guidance for further diagnostic workup and treatment. AJR Am J Roentgenol 2007;188:57–68.

8. Devaraj A, Cook GJ, Hansell DM. PET/CT in non-small cell lung cancer staging-promises and problems. Clin Radiol 2007;62:97–108.
9. Erasmus JJ, Connolly JE, McAdams HP, Roggli VL. Solitary pulmonary nodules: Part I. Morphologic evaluation for differentiation of benign and malignant lesions. Radiographics 2000;20:43–58.
10. Lee KS, Yi CA, Jeong SY, et al. Solid or partly solid solitary pulmonary nodules: their characterization using contrast wash-in and morphologic features at helical CT. Chest 2007;131:1516–1525.
11. Yi CA, Lee KS, Kim BT, et al. Tissue characterization of solitary pulmonary nodule: comparative study between helical dynamic CT and integrated PET/CT. J Nucl Med 2006;47:443–450.
12. Erasmus JJ, McAdams HP, Connolly JE. Solitary pulmonary nodules: Part II. Evaluation of the indeterminate nodule. Radiographics 2000; 20:59–66.
13. Goo JM, Im JG, Do KH, et al. Pulmonary tuberculoma evaluated by means of FDG PET: findings in 10 cases. Radiology 2000;216:117–121.
14. Erasmus JJ, McAdams HP, Patz EF Jr, Coleman RE, Ahuja V, Goodman PC. Evaluation of primary pulmonary carcinoid tumors using FDG PET. AJR Am J Roentgenol 1998;170:1369–1373.
15. Higashi K, Ueda Y, Seki H, et al. Fluorine-18-FDG PET imaging is negative in bronchioloalveolar lung carcinoma. J Nucl Med 1998;39: 1016–1020.
16. Lee HY, Choi YL, Lee KS, et al. Pure ground-glass opacity neoplastic lung nodules: histopathology, imaging, and management. AJR Am J Roentgenol 2014;202:W224–233.
17. Lee HY, Jeong JY, Lee KS, et al. Solitary pulmonary nodular lung adenocarcinoma: correlation of histopathologic scoring and patient survival with imaging biomarkers. Radiology 2012;264:884–893.
18. Lee HY, Lee KS, Han J, et al. Mucinous versus nonmucinous solitary pulmonary nodular bronchioloalveolar carcinoma: CT and FDG PET findings and pathologic comparisons. Lung Cancer 2009;65:170–175.
19. Kim HY, Shim YM, Lee KS, Han J, Yi CA, Kim YK. Persistent pulmonary nodular ground-glass opacity at thin-section CT: histopathologic comparisons. Radiology 2007;245:267–275.
20. Jeong SY, Lee KS, Shin KM, et al. Efficacy of PET/CT in the characterization of solid or partly solid solitary pulmonary nodules. Lung Cancer 2008;61:186–194.
21. Vesselle H, Salskov A, Turcotte E, et al. Relationship between non-small cell lung cancer FDG uptake at PET, tumor histology, and Ki-67 proliferation index. J Thorac Oncol 2008;3:971–978.
22. Dooms C, van Baardwijk A, Verbeken E, et al. Association between 18F-fluoro-2-deoxy-D-glucose uptake values and tumor vitality: prognostic value of positron emission tomography in early-stage non-small cell lung cancer. J Thorac Oncol 2009;4:822–828.
23. Hoang JK, Hoagland LF, Coleman RE, Coan AD, Herndon JE, 2nd, Patz EF Jr. Prognostic value of fluorine-18 fluorodeoxyglucose positron emission tomography imaging in patients with advanced-stage non-small-cell lung carcinoma. J Clin Oncol 2008;26:1459–1464.
24. Vesselle H, Freeman JD, Wiens L, et al. Fluorodeoxyglucose uptake of primary non-small cell lung cancer at positron emission tomography: new contrary data on prognostic role. Clin Cancer Res 2007;13: 3255–3263.
25. Hyun SH, Ahn HK, Kim H, et al. Volume-based assessment by (18)F-FDG PET/CT predicts survival in patients with stage III non-small-cell lung cancer. Eur J Nucl Med Mol Imaging 2014;41:50–58.
26. Park GC, Kim JS, Roh JL, Choi SH, Nam SY, Kim SY. Prognostic value of metabolic tumor volume measured by 18F-FDG PET/CT in advanced-stage squamous cell carcinoma of the larynx and hypopharynx. Ann Oncol 2013;24:208–214.
27. Song MK, Chung JS, Shin HJ, et al. Prognostic value of metabolic tumor volume on PET / CT in primary gastrointestinal diffuse large B cell lymphoma. Cancer Sci 2012;103:477–482.
28. Chung HH, Kwon HW, Kang KW, et al. Prognostic value of preoperative metabolic tumor volume and total lesion glycolysis in patients with epithelial ovarian cancer. Ann Surg Oncol 2012;19: 1966–1972.
29. Green S, Weiss GR. Southwest Oncology Group standard response criteria, endpoint definitions and toxicity criteria. Investig New Drugs 1992;10:239–253.
30. Werner-Wasik M, Xiao Y, Pequignot E, Curran WJ, Hauck W. Assessment of lung cancer response after nonoperative therapy: tumor diameter, bidimensional product, and volume. A serial CT scan-based study. Int J Radiat Oncol Biol Phys 2001;51:56–61.
31. Mac Manus MP, Hicks RJ, Matthews JP, et al. Positron emission tomography is superior to computed tomography scanning for response-assessment after radical radiotherapy or chemoradiotherapy in patients with non-small-cell lung cancer. J Clin Oncol 2003;21: 1285–1292.
32. Wahl RL, Jacene H, Kasamon Y, Lodge MA. From RECIST to PERCIST: Evolving Considerations for PET response criteria in solid tumors. J Nucl Med 2009;50(Suppl 1):122S–150S.
33. Brix G, Lechel U, Glatting G, et al. Radiation exposure of patients undergoing whole-body dual-modality 18F-FDG PET/CT examinations. J Nucl Med 2005;46:608–613.
34. Ackman JB, Wu CC, Halpern EF, Abbott GF, Shepard JA. Nonvascular thoracic magnetic resonance imaging: the current state of training, utilization, and perceived value: survey of the Society of Thoracic Radiology Membership. J Thorac Imaging 2014;29:252–257.
35. Biederer J, Beer M, Hirsch W, et al. MRI of the lung (2/3). Why ... when ... how? Insights Imaging 2012;3:355–371.
36. Boiselle PM, Biederer J, Gefter WB, Lee EY. Expert opinion: why is MRI still an under-utilized modality for evaluating thoracic disorders? J Thorac Imaging 2013;28:137.
37. Biederer J, Mirsadraee S, Beer M, et al. MRI of the lung (3/3)-current applications and future perspectives. Insights Imaging 2012;3:373–386.
38. Wild JM, Marshall H, Bock M, et al. MRI of the lung (1/3): methods. Insights Imaging 2012;3:345–353.
39. Puderbach M, Hintze C, Ley S, Eichinger M, Kauczor HU, Biederer J. MR imaging of the chest: a practical approach at 1.5T. Eur J Radiol 2007;64:345–355.
40. Fink C, Puderbach M, Biederer J, et al. Lung MRI at 1.5 and 3 Tesla: observer preference study and lesion contrast using five different pulse sequences. Invest Radiol 2007;42:377–383.
41. Edelstein WA, Glover GH, Hardy CJ, Redington RW. The intrinsic signal-to-noise ratio in NMR imaging. Magn Reson Med 1986;3:604–618.
42. Regier M, Kandel S, Kaul MG, et al. Detection of small pulmonary nodules in high-field MR at 3 T: evaluation of different pulse sequences using porcine lung explants. Eur Radiol 2007;17:1341–1351.
43. Attenberger UI, Ingrisch M, Dietrich O, et al. Time-resolved 3D pulmonary perfusion MRI: comparison of different k-space acquisition strategies at 1.5 and 3 T. Invest Radiol 2009;44:525–531.
44. Fabel M, Wintersperger BJ, Dietrich O, et al. MRI of respiratory dynamics with 2D steady-state free-precession and 2D gradient echo sequences at 1.5 and 3 Tesla: an observer preference study. Eur Radiol 2009;19:391–399.
45. Biederer J, Schoene A, Freitag S, Reuter M, Heller M. Simulated pulmonary nodules implanted in a dedicated porcine chest phantom: sensitivity of MR imaging for detection. Radiology 2003;227:475–483.
46. Both M, Schultze J, Reuter M, et al. Fast T1- and T2-weighted pulmonary MR-imaging in patients with bronchial carcinoma. Eur J Radiol 2005;53:478–488.
47. Bruegel M, Gaa J, Woertler K, et al. MRI of the lung: value of different turbo spin-echo, single-shot turbo spin-echo, and 3D gradient-echo pulse sequences for the detection of pulmonary metastases. J Magn Reson Imaging JMRI 2007;25:73–81.
48. Heye T, Ley S, Heussel CP, et al. Detection and size of pulmonary lesions: how accurate is MRI? A prospective comparison of CT and MRI. Acta Radiol 2012;53:153–160.

49. Regier M, Schwarz D, Henes FO, et al. Diffusion-weighted MR-imaging for the detection of pulmonary nodules at 1.5 Tesla: intraindividual comparison with multidetector computed tomography. J Med Imaging Radiat Oncol 2011;55:266–274.

50. Koyama H, Ohno Y, Aoyama N, et al. Comparison of STIR turbo SE imaging and diffusion-weighted imaging of the lung: capability for detection and subtype classification of pulmonary adenocarcinomas. Eur Radiol 2010;20:790–800.

51. Gamsu G, de Geer G, Cann C, Muller N, Brito A. A preliminary study of MRI quantification of simulated calcified pulmonary nodules. Invest Radiol 1987;22:853–858.

52. Wu NY, Cheng HC, Ko JS, et al. Magnetic resonance imaging for lung cancer detection: experience in a population of more than 10,000 healthy individuals. BMC Cancer 2011;11:242.

53. Shioya S, Haida M, Ono Y, Fukuzaki M, Yamabayashi H. Lung cancer: differentiation of tumor, necrosis, and atelectasis by means of T1 and T2 values measured in vitro. Radiology 1988;167:105–109.

54. Koyama H, Ohno Y, Kono A, et al. Quantitative and qualitative assessment of non-contrast-enhanced pulmonary MR imaging for management of pulmonary nodules in 161 subjects. Eur Radiol 2008; 18:2120–2131.

55. Gaeta M, Ascenti G, Mazziotti S, Contiguglia R, Barone M, Mileto A. MRI differentiation of pneumonia-like mucinous adenocarcinoma and infectious pneumonia. Eur J Radiol 2012;81:3587–3591.

56. Sakai F, Sone S, Kiyono K, et al. MR of pulmonary hamartoma: pathologic correlation. J Thorac Imaging 1994;9:51–55.

57. Razek AA, Fathy A, Gawad TA. Correlation of apparent diffusion coefficient value with prognostic parameters of lung cancer. J Comput Assist Tomogr 2011;35:248–252.

58. Takenaka D, Ohno Y, Hatabu H, et al. Differentiation of metastatic versus non-metastatic mediastinal lymph nodes in patients with non-small cell lung cancer using respiratory-triggered short inversion time inversion recovery (STIR) turbo spin-echo MR imaging. Eur J Radiol 2002;44:216–224.

59. Wu LM, Xu JR, Hua J, et al. Can diffusion-weighted imaging be used as a reliable sequence in the detection of malignant pulmonary nodules and masses? Magn Reson Imaging 2013;31:235–246.

60. Chang Q, Wu N, Ouyang H, Huang Y. Diffusion-weighted magnetic resonance imaging of lung cancer at 3.0 T: a preliminary study on monitoring diffusion changes during chemoradiation therapy. Clin Imaging 2012;36:98–103.

61. Tsuchida T, Morikawa M, Demura Y, Umeda Y, Okazawa H, Kimura H. Imaging the early response to chemotherapy in advanced lung cancer with diffusion-weighted magnetic resonance imaging compared to fluorine-18 fluorodeoxyglucose positron emission tomography and computed tomography. J Magn Reson Imaging JMRI 2013;38:80–88.

62. Yabuuchi H, Hatakenaka M, Takayama K, et al. Non-small cell lung cancer: detection of early response to chemotherapy by using contrast-enhanced dynamic and diffusion-weighted MR imaging. Radiology 2011;261:598–604.

63. Ohba Y, Nomori H, Mori T, Shiraishi K, Namimoto T, Katahira K. Diffusion-weighted magnetic resonance for pulmonary nodules: 1.5 vs. 3 Tesla. Asian Cardiovasc Thorac Ann 2011;19:108–114.

64. Ohno Y, Koyama H, Takenaka D, et al. Dynamic MRI, dynamic multidetector-row computed tomography (MDCT), and coregistered 2-[fluorine-18]-fluoro-2-deoxy-D-glucose-positron emission tomography (FDG-PET)/CT: comparative study of capability for management of pulmonary nodules. J Magn Reson Imaging JMRI 2008;27:1284–1295.

65. Satoh S, Nakaminato S, Kihara A, Isogai S, Kawai S. Evaluation of indeterminate pulmonary nodules with dynamic MR imaging. Magn Reson Med Sci 2013;12:31–38.

66. Schaefer JF, Schneider V, Vollmar J, et al. Solitary pulmonary nodules: association between signal characteristics in dynamic contrast enhanced MRI and tumor angiogenesis. Lung Cancer 2006;53:39–49.

67. Kono R, Fujimoto K, Terasaki H, et al. Dynamic MRI of solitary pulmonary nodules: comparison of enhancement patterns of malignant and benign small peripheral lung lesions. AJR Am J Roentgenol 2007;188: 26–36.

68. Chang YC, Yu CJ, Chen CM, et al. Dynamic contrast-enhanced MRI in advanced nonsmall-cell lung cancer patients treated with first-line bevacizumab, gemcitabine, and cisplatin. J Magn Reson Imaging JMRI 2012;36:387–396.

69. Pauls S, Breining T, Muche R, et al. The role of dynamic, contrast-enhanced MRI in differentiating lung tumor subtypes. Clin Imaging 2011;35:259–265.

70. Puderbach M, Risse F, Biederer J, et al. In vivo Gd-DTPA concentration for MR lung perfusion measurements: assessment with computed tomography in a porcine model. Eur Radiol 2008;18:2102–2107.

71. Henzler T, Konstandin S, Schmid-Bindert G, et al. Imaging of tumor viability in lung cancer: initial results using 23Na-MRI. RoFo 2012;184: 340–344.

72. Pichler BJ, Kolb A, Nagele T, Schlemmer HP. PET/MRI: paving the way for the next generation of clinical multimodality imaging applications. J Nucl Med 2010;51:333–336.

73. Stolzmann P, Veit-Haibach P, Chuck N, et al. Detection rate, location, and size of pulmonary nodules in trimodality PET/CT-MR: comparison of low-dose CT and Dixon-based MR imaging. Invest Radiol 2013;48: 241–246.

74. Schmidt H, Brendle C, Schraml C, et al. Correlation of simultaneously acquired diffusion-weighted imaging and 2-deoxy-[18F] fluoro-2-D-glucose positron emission tomography of pulmonary lesions in a dedicated whole-body magnetic resonance/positron emission tomography system. Invest Radiol 2013;48:247–255.

75. Chandarana H, Heacock L, Rakheja R, et al. Pulmonary nodules in patients with primary malignancy: comparison of hybrid PET/MR and PET/CT imaging. Radiology 2013;268:874–881.

76. Antoch G, Vogt FM, Freudenberg LS, et al. Whole-body dual-modality PET/CT and whole-body MRI for tumor staging in oncology. JAMA 2003;290:3199–3206.

77. Chen YQ, Yang Y, Xing YF, Jiang S, Sun XW. Detection of rib metastases in patients with lung cancer: a comparative study of MRI, CT and bone scintigraphy. PLoS One 2012;7:e52213.

78. Dinkel J, Khalilzadeh O, Hintze C, et al. Inter-observer reproducibility of semi-automatic tumor diameter measurement and volumetric analysis in patients with lung cancer. Lung Cancer 2013;82:76–82.

79. Biederer J, Hintze C, Fabel M, Dinkel J. Magnetic resonance imaging and computed tomography of respiratory mechanics. J Magn Reson Imaging JMRI 2010;32:1388–1397.

80. Wurslin C, Schmidt H, Martirosian P, et al. Respiratory motion correction in oncologic PET using T1-weighted MR imaging on a simultaneous whole-body PET/MR system. J Nucl Med 2013;54:464–471.

81. Becker N, Motsch E, Gross ML, et al. Randomized study on early detection of lung cancer with MSCT in Germany: study design and results of the first screening round. J Cancer Res Clin Oncol 2012; 138:1475–1486.

82. Sommer G, Tremper J, Koenigkam-Santos M, et al. Lung nodule detection in a high-risk population: comparison of magnetic resonance imaging and low-dose computed tomography. Eur J Radiol 2014;83:600–605.

83. National Lung Screening Trial Research Team; Aberle DR, Adams AM, et al. Reduced lung-cancer mortality with low-dose computed tomographic screening. N Engl J Med 2011;365:395–409.

84. Brenner DJ. Radiation risks potentially associated with low-dose CT screening of adult smokers for lung cancer. Radiology 2004;231:440–445.

85. Rami-Porta R, Crowley JJ, Goldstraw P. The revised TNM staging system for lung cancer. Ann Thorac Cardiovasc Surg 2009;15:4–9.

86. Robinson LA, Ruckdeschel JC, Wagner H Jr, et al. Treatment of non-small cell lung cancer-stage IIIA: ACCP evidence-based clinical practice guidelines (2nd edition). Chest 2007;132:243S–265S.

87. Pisters KM. Adjuvant chemotherapy for non-small-cell lung cancer—the smoke clears. N Engl J Med 2005;352:2640–2642.

88. Halpern BS, Schiepers C, Weber WA, et al. Presurgical staging of non-small cell lung cancer: positron emission tomography, integrated positron emission tomography/CT, and software image fusion. Chest 2005;128:2289–2297.

89. Kim YK, Lee HY, Lee KS, et al. Dry pleural dissemination in non-small cell lung cancer: prognostic and diagnostic implications. Radiology 2011;260:568–574.

90. Lardinois D, Weder W, Hany TF, et al. Staging of non-small-cell lung cancer with integrated positron-emission tomography and computed tomography. N Engl J Med 2003;348:2500–2507.

91. Pieterman RM, van Putten JW, Meuzelaar JJ, et al. Preoperative staging of non-small-cell lung cancer with positron-emission tomography. N Engl J Med 2000;343:254–261.

92. Shim SS, Lee KS, Kim BT, et al. Integrated PET/CT and the dry pleural dissemination of peripheral adenocarcinoma of the lung: diagnostic implications. J Comput Assist Tomogr 2006;30:70–76.

93. Shim SS, Lee KS, Kim BT, et al. Non-small cell lung cancer: prospective comparison of integrated FDG PET/CT and CT alone for preoperative staging. Radiology 2005;236:1011–1019.

94. Foroulis CN, Zarogoulidis P, Darwiche K, et al. Superior sulcus (Pancoast) tumors: current evidence on diagnosis and radical treatment. J Thorac Dis 2013;5(Suppl 4):S342–358.

95. Yi CA, Lee KS, Lee HY, et al. Coregistered whole body magnetic resonance imaging-positron emission tomography (MRI-PET) versus PET-computed tomography plus brain MRI in staging resectable lung cancer: comparisons of clinical effectiveness in a randomized trial. Cancer 2013;119:1784–1791.

96. Deslauriers J, Gregoire J. Clinical and surgical staging of non-small cell lung cancer. Chest 2000;117:96S–103S.

97. van Tinteren H, Hoekstra OS, Smit EF, et al. Effectiveness of positron emission tomography in the preoperative assessment of patients with suspected non-small-cell lung cancer: the PLUS multicentre randomised trial. Lancet 2002;359:1388–1393.

98. Schrevens L, Lorent N, Dooms C, Vansteenkiste J. The role of PET scan in diagnosis, staging, and management of non-small cell lung cancer. Oncologist 2004;9:633–643.

99. Magnani P, Carretta A, Rizzo G, et al. FDG/PET and spiral CT image fusion for medistinal lymph node assessment of non-small cell lung cancer patients. J Cardiovasc Surg 1999;40:741–748.

100. Vansteenkiste JF, Stroobants SG, Dupont PJ, et al. FDG-PET scan in potentially operable non-small cell lung cancer: do anatometabolic PET-CT fusion images improve the localisation of regional lymph node metastases? The Leuven Lung Cancer Group. Eur J Nucl Med 1998;25:1495–1501.

101. Wahl RL, Quint LE, Greenough RL, Meyer CR, White RI, Orringer MB. Staging of mediastinal non-small cell lung cancer with FDG PET, CT, and fusion images: preliminary prospective evaluation. Radiology 1994;191:371–377.

102. Sung YM, Lee KS, Kim BT, et al. Nonpalpable supraclavicular lymph nodes in lung cancer patients: preoperative characterization with 18F-FDG PET/CT. AJR Am J Roentgenol 2008;190:246–252.

103. Hintze C, Biederer J, Wenz HW, Eberhardt R, Kauczor HU. [MRI in staging of lung cancer.] Radiologe 2006;46:251–254, 256–259.

104. Hasegawa I, Boiselle PM, Kuwabara K, Sawafuji M, Sugiura H. Mediastinal lymph nodes in patients with non-small cell lung cancer: preliminary experience with diffusion-weighted MR imaging. J Thorac Imaging 2008;23:157–161.

105. Pauls S, Schmidt SA, Juchems MS, et al. Diffusion-weighted MR imaging in comparison to integrated [(1)(8)F]-FDG PET/CT for N-staging in patients with lung cancer. Eur J Radiol 2012;81:178–182.

106. Nomori H, Mori T, Ikeda K, et al. Diffusion-weighted magnetic resonance imaging can be used in place of positron emission tomography for N staging of non-small cell lung cancer with fewer false-positive results. J Thorac Cardiovasc Surg 2008;135:816–822.

107. Usuda K, Zhao XT, Sagawa M, et al. Diffusion-weighted imaging is superior to positron emission tomography in the detection and nodal assessment of lung cancers. Ann Thorac Surg 2011;91:1689–1695.

108. Wu LM, Xu JR, Gu HY, et al. Preoperative mediastinal and hilar nodal staging with diffusion-weighted magnetic resonance imaging and fluorodeoxyglucose positron emission tomography/computed tomography in patients with non-small-cell lung cancer: which is better? J Surg Res 2012;178:304–314.

109. Morikawa M, Demura Y, Ishizaki T, et al. The effectiveness of 18F-FDG PET/CT combined with STIR MRI for diagnosing nodal involvement in the thorax. J Nucl Med 2009;50:81–87.

110. Ohno Y, Hatabu H, Takenaka D, et al. Metastases in mediastinal and hilar lymph nodes in patients with non-small cell lung cancer: quantitative and qualitative assessment with STIR turbo spin-echo MR imaging. Radiology 2004;231:872–879.

111. Ohno Y, Koyama H, Yoshikawa T, et al. N stage disease in patients with non-small cell lung cancer: efficacy of quantitative and qualitative assessment with STIR turbo spin-echo imaging, diffusion-weighted MR imaging, and fluorodeoxyglucose PET/CT. Radiology 2011;261:605–615.

112. Weder W, Schmid RA, Bruchhaus H, Hillinger S, von Schulthess GK, Steinert HC. Detection of extrathoracic metastases by positron emission tomography in lung cancer. Ann Thorac Surg 1998;66:886–892; discussion 892–883.

113. Saunders CA, Dussek JE, O'Doherty MJ, Maisey MN. Evaluation of fluorine-18-fluorodeoxyglucose whole body positron emission tomography imaging in the staging of lung cancer. Ann Thorac Surg 1999;67:790–797.

114. Stroobants SG, D'Hoore I, Dooms C, et al. Additional value of whole-body fluorodeoxyglucose positron emission tomography in the detection of distant metastases of non-small-cell lung cancer. Clin Lung Cancer 2003;4:242–247.

115. Barkhausen J, Quick HH, Lauenstein T, et al. Whole-body MR imaging in 30 seconds with real-time true FISP and a continuously rolling table platform: feasibility study. Radiology 2001;220:252–256.

116. Lauenstein TC, Goehde SC, Herborn CU, et al. Whole-body MR imaging: evaluation of patients for metastases. Radiology 2004;233:139–148.

117. Schlemmer HP, Schafer J, Pfannenberg C, et al. Fast whole-body assessment of metastatic disease using a novel magnetic resonance imaging system: initial experiences. Invest Radiol 2005;40:64–71.

118. Yi CA, Shin KM, Lee KS, et al. Non-small cell lung cancer staging: efficacy comparison of integrated PET/CT versus 3.0-T whole-body MR imaging. Radiology 2008;248:632–642.